$\mathscr{L}_1$ Adaptive Control for Autonomous Rotorcraft

B. J. Guerreiro* , C. Silvestre*, R. Cunha*, C. Cao†, N. Hovakimyan‡

***Abstract*— In this paper, the $\mathscr{L}_1$ adaptive control theory is used to design a high bandwidth inner loop controller to provide attitude and velocity stabilization of an autonomous small-scale rotorcraft in the presence of wind disturbances. The nonlinear model of the vehicle is expressed as a linear time-varying system for a predefined region of operation, for which an $\mathscr{L}_1$ adaptive controller is designed. The $\mathscr{L}_1$ adaptive controller ensures that an uncertain linear time-varying system has uniformly bounded transient response for system's input and output signals, in addition to stable tracking. The performance bounds of $\mathscr{L}_1$ adaptive controller can be systematically improved by increasing the adaptation rate without hurting the robustness of the system. The performance achieved with the $\mathscr{L}_1$ controller is compared with that obtained via a linear state feedback controller for demanding reference signals in the presence of wind disturbances. Simulation results show that the performance of the $\mathscr{L}_1$ surpasses that of the linear controller illustrating the advantages of fast adaptation.**

I. INTRODUCTION

Within the scope of Unmanned Aerial Vehicles, autonomous rotorcraft have been steadily growing as a major topic of research. They have the potential to perform high precision tasks in challenging and uncertain operation scenarios as new sensor technology and increasingly powerful and low cost computational systems are becoming available. Nonetheless, their highly nonlinear, coupled, unstable and fast dynamics represent a challenge for the control engineering community. For instance, in [1] a trajectory tracking $\mathscr{H}_2$ gain scheduling methodology is used to control an autonomous rotorcraft subject to wind disturbance.

In this paper, the $\mathscr{L}_1$ control theory, introduced in [2], [3], [4], [5] and generalized for multi-input multi-output (MIMO) systems in [6], is used to design a high bandwidth inner loop controller to provide attitude and velocity stabilization of an autonomous small-scale helicopter. Thus, the $\mathscr{L}_1$ adaptive control theory is applied to a nonlinear dynamic model of a small-scale helicopter to achieve velocity tracking by adapting to different points of operation. The $\mathscr{L}_1$ adaptive controller ensures that an uncertain linear system has uniformly bounded transient and asymptotic tracking for system's input and output signals. The performance bounds of the $\mathscr{L}_1$ adaptive controller can be systematically improved by increasing the adaptation rate, without compromising the robustness of the closed-loop system. The performance of the $\mathscr{L}_1$ controller is compared, in a realistic simulation environment, with that achieved by the nominal controller used in the specification of the reference system, which follows from [1]. The wind disturbance, which uses Von Karman disturbance models and wind gusts, leads the vehicle outside the predefined region of operation. The vehicle model used in the simulation is the full nonlinear model of the helicopter.

This paper is organized as follows: Section II briefly presents the helicopter dynamic model and the reformulation of this model into the standard $\mathscr{L}_1$ design setup. Section III formulates the $\mathscr{L}_1$ adaptive control problem and the main results from the $\mathscr{L}_1$ theory are presented. In Section IV the implementation details and the simulation results are presented and discussed; and finally, Section V summarizes the main conclusions and points out directions for further work.

II. HELICOPTER MODEL

This section summarizes the dynamical model of the helicopter. A comprehensive coverage of helicopter flight dynamics can be found in [7]. In [8], [9] the model presented bellow is described in further detail.

Consider the helicopter, modeled as a rigid body, where the resultant force and moment applied to the helicopter's center of mass are the sum of the contributions of the helicopter components and gravitational force. Let $\left({}^{I}\mathbf{p}_B, {}^{I}_{B}R\right) \in SE(3) \triangleq \mathbb{R}^3 \times SO(3)$ denote the configuration of the body frame $\{B\}$ (attached to the vehicle's center of mass) with respect to the inertial frame $\{I\}$. Consider also the Z-Y-X Euler angles $\lambda_B = \left[\begin{array}{ccc} \phi_B & \theta_B & \psi_B \end{array}\right]'$, $\theta_B \in]-\frac{\pi}{2}, \frac{\pi}{2}[$, $\phi_B, \psi_B \in \mathbb{R}$, representing the orientation of $\{B\}$ relative to $\{I\}$ such that ${}^{I}_{B}R = \mathscr{R}(\lambda_B)$. In addition, let $\mathbf{v}_B$ and ω_B denote the linear and angular body velocities, respectively. For the sake of simplicity, the time dependence of the state, input and disturbance vectors are omitted within the description of the helicopter nonlinear model. Using these notations, the state equations of the helicopter dynamics can be written as

$$\left\{\begin{array}{rcl} \dot{\mathbf{v}}_B & = & -\omega_B \times \mathbf{v}_B + \frac{1}{m}\left[\mathbf{f}_e\left(\mathbf{v}_B, \omega_B, \mathbf{u}_B, \mathbf{v}_w\right) + \mathbf{f}_g\left(\phi_B, \theta_B\right)\right] \\ \dot{\omega}_B & = & -I_B^{-1}\left(\omega_B \times I_B\, \omega_B\right) + I_B^{-1}\, \mathbf{n}_e\left(\mathbf{v}_B, \omega_B, \mathbf{u}_B, \mathbf{v}_w\right) \\ \Pi\dot{\lambda}_B & = & \Pi\, \mathscr{Q}\left(\phi_B, \theta_B\right) \omega_B \end{array}\right. \tag{1}$$

* Instituto Superior Tecnico, Institute for Systems and Robotics, Av. Rovisco Pais, 1, 1049-001 Lisboa, Portugal, {bguerreiro,cjs,rita}@isr.ist.utl.pt.

†Department of Mechanical Engineering, University of Connecticut, 191 Auditorium Road, Unit 3139, Storrs, CT 06269, USA, ccao@engr.uconn.edu.

‡Mechanical Science and Engineering, University of Illinois at Urbana-Champaign, 223 Mechanical Engineering Building, MC-244 1206, West Green street, Urbana, IL 61801, USA, nhovakim@illinois.edu

This work was partially supported by Fundação para a Ciência e a Tecnologia (ISR/IST pluriannual funding) through the POS_Conhecimento Program that includes FEDER funds and by the PTDC/EEA-ACR/72853/2006 HELICIM project. The work of B. J. Guerreiro was supported by the PhD Student Grant SFRH/BD/21781/2005 from the Portuguese FCT POCTI programme. The work of N. Hovakimyan is supported by AFOSR under Contract No. FA9550-08-1-0135.

where m is the vehicle mass, I_B is the tensor of inertia about the frame $\{B\}$, $\mathbf{u}_B$ is the input vector, $\mathbf{v}_w$ is the wind velocity disturbance, $\mathbf{f}_e$, $\mathbf{n}_e$, and $\mathbf{f}_g$ are the external force, moment, and gravitational force, respectively, all expressed in the body frame, $\mathscr{Q}$ is the transformation from angular rates to Euler angle derivatives and $\Pi = \begin{bmatrix} 1 & 0 & 0 \\ 0 & 1 & 0 \end{bmatrix}$. The state vector $\mathbf{x}_B = [\mathbf{v}_B' \; \omega_B' \; \Pi\lambda_B']' \in \mathscr{X} \subset \mathbb{R}^{n_x}$ has dimension $n_x = 8$. The input vector $\mathbf{u}_B \in \mathscr{U} \subset \mathbb{R}^{n_u}$ with $n_u = 4$, defined as $\mathbf{u}_B = \begin{bmatrix} \theta_{c_0} & \theta_{c_{1c}} & \theta_{c_{1s}} & \theta_{c_{0t}} \end{bmatrix}'$, comprises the main rotor collective input θ_{c_0}, the main rotor cyclic inputs $\theta_{c_{1c}}$ and $\theta_{c_{1s}}$, and the tail rotor collective input $\theta_{c_{0t}}$.

The force and moment vectors can be decomposed as $\mathbf{f}_e = \mathbf{f}_{mr} + \mathbf{f}_{tr} + \mathbf{f}_{fus} + \mathbf{f}_{tp} + \mathbf{f}_{fn}$ and $\mathbf{n}_e = \mathbf{n}_{mr} + \mathbf{n}_{tr} + \mathbf{n}_{fus} + \mathbf{n}_{tp} + \mathbf{n}_{fn}$, where the subscripts mr, tr, fus, tp and fn stand for the contributions of the main rotor, tail rotor, fuselage, horizontal tail plane and vertical tail fin, respectively.

A. Main Rotor

As the primary source of lift, propulsion and control, the main rotor dominates the helicopter dynamic behavior. As a result of the aerodynamic lift forces that are generated at the surface of its rotating blades, the main rotor is responsible for the helicopter's distinctive ability to operate in low-speed regimes, which include hovering and vertical maneuvering.

To present the main rotor equations of motion, the following frame needs to be introduced:

> $\{hw\}$ – Hub/Wind frame. Non-rotating frame, with its origin at the hub, x-axis aligned with the component of the helicopter linear velocity relative to the fluid that is parallel with the hub plane.

Most of the helicopter maneuvering capabilities result from effectively controlling the main rotor aerodynamic loads. This is achieved by means of the swashplate - a mechanism responsible for applying a different blade pitch angle θ_{mr} at each blade azimuth angle ψ_m, such that $\theta_{mr}(\psi_m) = \theta_{c_0} + \theta_{1c}\cos\psi_m + \theta_{1s}\sin\psi_m$. The collective command θ_{c_0} is directly applied to the main rotor blades, whereas the cyclics θ_{1c} and θ_{1s} result from combining the cyclic commands $\theta_{c_{1c}}$ and $\theta_{c_{1s}}$ with the flapping motion of the Bell-Hiller stabilizing bar, also called flybar. This combined motion can be described by the first order system

$$\Omega A_{\dot{\theta}}\,\dot{\theta}_1 + \Omega^2 A_\theta(\mu)\,\theta_1 = \Omega^2\left(B_\theta(\mu)\,\theta_{c_1} + B_\omega\,\omega + B_\lambda(\mu)\,\lambda\right) \tag{2}$$

where $\theta_1 = \begin{bmatrix} \theta_{1c} & \theta_{1s} \end{bmatrix}'$, $\theta_{c_1} = \begin{bmatrix} \theta_{c_{1c}} & \theta_{c_{1s}} \end{bmatrix}'$, $\omega = \begin{bmatrix} \bar{p} & \bar{q} \end{bmatrix}'$, $\lambda = \begin{bmatrix} \mu_z - \lambda_0 & \lambda_{1c} & \lambda_{1s} \end{bmatrix}'$ and $\Omega = \dot{\psi}_m$ is the rotor speed. The variables μ and μ_z are the normalized x and z-components of the hub linear velocity and $\bar{p}$ and $\bar{q}$ are the normalized x and y-components of the angular velocity, all expressed in the frame $\{hw\}$. Detailed expressions for the matrices $A_{\dot{\theta}}$, $A_\theta(\mu)$, $B_\theta(\mu)$, B_ω, and $B_\lambda(\mu)$ can be found in [9]. In the present work, the dynamics of the pitching mechanism are neglected, $\dot{\theta}_1 = 0$, considering only the steady-state equations.

As result of the thrust force generated at the surface of the rotating blades, the air is accelerated downwards creating a flowfield, usually called induced downwash. The downwash can be decomposed in Fourier Series and approximated by the constant and first-order harmonic terms, yielding an expression similar to that of the blade pitch angle $\lambda(\psi_m) = \lambda_0 + r_m(\lambda_{1c}\cos\psi_m + \lambda_{1s}\sin\psi_m)$, where r_m is the rotor radius integration variable. Also as a consequence of the rotation and feathering (blade pitching) motions and interaction with the motion of the helicopter, the blades describe flap and lag motions, roughly characterized by pulling up and backwards, respectively, the tip of the blade. In this work, assuming that the blades are rigid and linked to the hub through flap hinge springs with stiffness k_β, the lag motion is neglected and the flap motion is approximated by the first three components of the Fourier Series expansion of the steady-state solution, that is,

$$\beta = A_0^{-1}(\mu)\left[B_1(\mu)\,\theta + B_2(\mu)\,\omega + B_3(\mu)\,\lambda\right] \tag{3}$$

where $\beta = \begin{bmatrix} \beta_0 & \beta_{1c} & \beta_{1s} \end{bmatrix}'$, $\theta = \begin{bmatrix} \theta_{c_0} & \theta_{1c} & \theta_{1s} \end{bmatrix}'$, and the matrices $A_0(\mu)$, $B_1(\mu)$, $B_2(\mu)$, and $B_3(\mu)$ are defined in [9].

The forces and moments generated by the main rotor are the sum of the contributions of each blade expressed in the hub frame. The main rotor contribution to the total force acting on the helicopter can be written as $\mathbf{f}_{mr} = {}^{B}_{hw}R\,{}^{hw}\mathbf{f}_{mr}$, with the expression for ${}^{hw}\mathbf{f}_{mr}$ given by

$${}^{hw}\mathbf{f}_{mr} \simeq \tfrac{n_b}{2}\begin{bmatrix} -Y_{1s} \\ -Y_{1c} \\ 2Z_0 \end{bmatrix} + \tfrac{n_b}{2}\begin{bmatrix} -Z_{1c} & -Z_0 - \dfrac{Z_{2c}}{2} & -\dfrac{Z_{2s}}{2} \\ Z_{1s} & \dfrac{Z_{2s}}{2} & Z_0 - \dfrac{Z_{2c}}{2} \\ 0 & 0 & 0 \end{bmatrix}\beta$$

where n_b is the number of blades, $Y_{(.)}$ and $Z_{(.)}$ are the components of the Fourier Series decomposition of the aerodynamic force generated at each blade. Similarly, the main rotor contribution to the overall moment is computed using $\mathbf{n}_{mr} = {}^{B}_{hw}R\,{}^{hw}\mathbf{n}_{mr}$, where the expression for ${}^{hw}\mathbf{n}_{mr}$ can be rewritten as

$${}^{hw}\mathbf{n}_{mr} \simeq n_b\begin{bmatrix} 0 \\ 0 \\ N_0 \end{bmatrix} + \tfrac{n_b}{2}\begin{bmatrix} -N_{1c} & -N_0 - \dfrac{N_{2c}}{2} & -k_\beta - \dfrac{N_{2s}}{2} \\ N_{1s} & -k_\beta + \dfrac{N_{2s}}{2} & N_0 - \dfrac{N_{2c}}{2} \\ 0 & 0 & 0 \end{bmatrix}\beta$$

and $N_{(.)}$ are the components of the Fourier Series decomposition of the aerodynamic yaw moment generated at each blade.

B. The Other Components

The tail rotor, placed at the tail boom in order to counteract the moment generated by the rotation of the main rotor, provides yaw control of the helicopter. To model this component we can use the same principles adopted for the main rotor, neglecting the blade flapping and pitching motions, which have little significance due to the small rotor size. The tail rotor contribution to the total force can be approximated by

$$\mathbf{f}_{tr} = {}^{B}_{tr}R^{tr}\mathbf{f} \simeq \begin{bmatrix} 0 \\ -n_{b_t}Z_{0_t} \\ 0 \end{bmatrix}, \tag{4}$$

where n_{b_t} is the number of blades of the tail rotor, Z_{0_t} is the thrust force produced by the tail rotor and ${}^{B}_{tr}R^{tr}$ is the

rotation from the tail rotor frame $\{tr\}$ to the body frame $\{B\}$. Similarly, the moment expression is given by

$$\mathbf{n}_{tr} = \begin{bmatrix} 0 \\ -n_{b_t} N_{0_t} \\ 0 \end{bmatrix} + {}^{B}\mathbf{p}_{tr} \times \mathbf{f}_{tr} \,, \tag{5}$$

where N_{0_t} is the tail rotor generated torque.

Accurate modeling of the aerodynamic forces and moments generated by the flow surrounding the helicopter fuselage is a demanding task. In this work these loads are modeled as functions of the mean flow speed v_{fus}, the incidence angle α_{fus} and the sideslip angle β_{fus}. The horizontal tail plane and vertical tail fin are modeled as normal wings, whose aerodynamic force contributions can be approximated by functions of the angle of attack and sideslip.

C. $\mathscr{L}_1$ Model Formulation

The nonlinear helicopter model presented above and denoted by the nonlinear dynamic equation

$$\dot{\mathbf{x}}_B(t) = \mathbf{f}(\mathbf{x}_B(t), \mathbf{u}_B(t), \mathbf{v}_w(t))$$

can be linearized along trajectories, considering $\mathbf{x}(t) = \mathbf{x}_B(t) - \mathbf{x}_C$, $\mathbf{u}(t) = \mathbf{u}_B(t) - \mathbf{u}_C$, with $\mathbf{x}_C$ and $\mathbf{u}_C$ as the state and input trimming values, respectively. A trimming trajectory of a helicopter can be described by a vector

$$\xi = [V_c \; \gamma_c \; \dot{\psi}_c \; \psi_{ct}]' \,, \tag{6}$$

that fully parameterizes the set of achievable helicopter trimming trajectories, which correspond to straight lines and z aligned helices described by the vehicle with arbitrary linear speed and yaw angle. Note that $V_c = \|\mathbf{v}_c\|$ is the linear body speed, γ_c the flight-path angle, $\dot{\psi}_c$ the angular velocity along the z-axis and ψ_{ct} the yaw angle difference between the tangent frame to the desired trajectory and the desired orientation.

It can be seen that, for a sufficiently small region of operation, the system can be approximated by a linear time-varying system of the form

$$\left\{ \begin{array}{rcl} \dot{\mathbf{x}}(t) & = & A(t)\mathbf{x}(t) + B_w \mathbf{w}(t) + B k_u \mathbf{u}(t) \\ \mathbf{y}(t) & = & C\mathbf{x}(t) \quad , \qquad \mathbf{x}(0) = \mathbf{x}_0 \end{array} \right. \tag{7}$$

where the matrix A can be decomposed in nominal and remaining parts, $A(t) = A_n + A_\delta(t)$, k_u is a positive constant and the term $B_w \mathbf{w}(t)$ accounts for uncertainties and wind disturbances. Thus, it can be seen that

$$\dot{\mathbf{x}}(t) = A_n \mathbf{x}(t) + B k_u \mathbf{u}(t) + B_w \mathbf{w}(t) + A_\delta(t)\mathbf{x}(t) \,. \tag{8}$$

Assumption 1: [Matching Assumption] There exists a control matrix K_n such that $A_m = A_n - BK_n$ is Hurwitz.

Assumption 2: There exist a time varying vector $\mathbf{k}_w(t)$ and a time varying matrix $K_\delta(t)$ such that $B(K_\delta(t)x(t) + \mathbf{k}_w(t)) = B_w \mathbf{w}(t) + A_\delta(t)\mathbf{x}(t)$.

Given the previous assumptions, and adding the zero valued term $B(K_n - K_n)\mathbf{x}(t)$ to the state equation and considering that $K_x(t) = K_n + K_\delta(t)$, the system equations can be written as

$$\left\{ \begin{array}{rcl} \dot{\mathbf{x}}(t) & = & A_m \mathbf{x}(t) + B(k_u \mathbf{u}(t) + K_x(t)\mathbf{x}(t) + \mathbf{k}_w(t)) \\ \mathbf{y}(t) & = & C\mathbf{x}(t) \quad , \qquad \mathbf{x}(0) = \mathbf{x}_0 \end{array} \right. , \tag{9}$$

where $k_u \in \mathscr{K}_u$ stands for the unknown control effectiveness, $K_x(t) \in \mathscr{K}_x$ and $\mathbf{k}_w(t) \in \mathscr{K}_w$. Without loss of generality it is assumed that

$$\mathscr{K}_u = \{k_u \in \mathbb{R} \mid k_u \in [\underline{k}_u, \bar{k}_u]\} \,,$$
$$\|\mathbf{k}_w(t)\| < \Delta_0 \,, \quad \forall \; t \geq 0 \,,$$

where $0 < \underline{k}_u < \bar{k}_u$ are known upper and lower bounds, $\Delta_0 \in \mathbb{R}^+$ is a known bound of $\mathbf{k}_w(t)$ and $\mathscr{K}_x$ is a known compact set. It is further assumed that $K_x(t)$ and $\mathbf{k}_w(t)$ are continuously differentiable and their derivatives are uniformly bounded, that is

$$\|\dot{K}_x(t)\|_2 \leq d_{Kx} < \infty \,, \quad \|\dot{\mathbf{k}}_w(t)\|_2 \leq d_{kw} < \infty \,, \quad \forall \; t \geq 0 \,,$$

where $\|.\|_2$ denotes the 2-norm, and d_{Kx}, d_{kw} can be arbitrarily large.

III. $\mathscr{L}_1$ ADAPTIVE CONTROLLER

In this section, the $\mathscr{L}_1$ adaptive control solution is presented for the rotorcraft linearized model. Recall that the plant model is described by

$$\left\{ \begin{array}{rcl} \dot{\mathbf{x}}(t) & = & A_m \mathbf{x}(t) + B(k_u \mathbf{u}(t) + K_x(t)\mathbf{x}(t) + \mathbf{k}_w(t)) \\ \mathbf{y}(t) & = & C\mathbf{x}(t), \qquad \mathbf{x}(0) = \mathbf{x}_0 \end{array} \right. . \tag{10}$$

The control objective is to design a state feedback adaptive controller for the system (10) to ensure that $\mathbf{y}(t)$ tracks a given bounded reference signal $\mathbf{r}(t)$, while all other error signals remain bounded.

The $\mathscr{L}_1$ adaptive controller is comprised of the state predictor, the adaptive laws and the control law, as detailed below. The state predictor is defined similar to the plant equations, but replacing the unknown variables by their estimates,

$$\left\{ \begin{array}{rcl} \dot{\hat{\mathbf{x}}}(t) & = & A_m \hat{\mathbf{x}}(t) + B\left(\hat{k}_u(t)\mathbf{u}(t) + \hat{K}_x(t)\mathbf{x}(t) + \hat{\mathbf{k}}_w(t)\right) \\ \hat{\mathbf{y}}(t) & = & C\hat{\mathbf{x}}(t) \quad , \qquad \hat{\mathbf{x}}(0) = \mathbf{x}_0 \end{array} \right. \tag{11}$$

where $\hat{k}_u(t)$, $\hat{K}_x(t)$, and $\hat{\mathbf{k}}_w(t)$ are the adaptive parameters computed using the adaptive laws given by

$$\left\{ \begin{array}{rcl} \dot{\hat{k}}_u(t) & = & \gamma \mathrm{Proj}(\hat{k}_u(t), B' P \tilde{\mathbf{x}}(t)\mathbf{u}'(t)) \\ \dot{\hat{K}}_x(t) & = & \gamma \mathrm{Proj}(\hat{K}_x(t), B' P \tilde{\mathbf{x}}(t)\mathbf{x}'(t)) \\ \dot{\hat{\mathbf{k}}}_w(t) & = & \gamma \mathrm{Proj}(\hat{\mathbf{k}}_w(t), B' P \tilde{\mathbf{x}}(t)) \end{array} \right. , \tag{12}$$

where $\tilde{\mathbf{x}} = \hat{\mathbf{x}} - \mathbf{x}$ is the prediction error state that results from the difference between the system (10) and the predictor (11), $\gamma > 0$ is the adaptation gain, $P = P' > 0$ is the matrix solution of the Lyapunov equation $A_m' P + P A_m = -Q$, with $Q > 0$, and $\mathrm{Proj}(.,.)$ denotes the projection operator, as defined in [10], generalized to parameter matrices.

The control law $\mathbf{u}(t)$ is generated as follows

$$\begin{array}{rcl} U(s) & = & -k_d D(s) \bar{R}(s) \\ \bar{\mathbf{r}}(t) & = & \hat{K}_x(t)\mathbf{x}(t) + \hat{k}_u(t)\mathbf{u}(t) + \hat{\mathbf{k}}_w(t) - K_g \mathbf{r}(t) \end{array} \tag{13}$$

where $k_d \in \mathbb{R}$, $K_g \in \mathbb{R}^{n_u \times n_u}$ and $D(s)$ is an $n_u \times n_u$ transfer function matrix that leads to a stable and strictly proper transfer function matrix $F(s)$ defined by

$$F(s) = (\mathbb{I} + k_u k_d D(s))^{-1} k_u k_d D(s) , \tag{14}$$

where $\mathbb{I}$ denotes the identity matrix of appropriate dimensions. Note that $\bar{R}(s) = \mathscr{L}\{\bar{\mathbf{r}}(t)\}$ stands for the Laplace transform of the signal $\bar{\mathbf{r}}(t)$, as well as $U(s) = \mathscr{L}\{\mathbf{u}(t)\}$.

To ensure the stability of the closed loop system with the $\mathscr{L}_1$ adaptive controller, the following conditions have to be satisfied by proper design of $D(s)$ and k_d:

$$(i)\ \ F(s) \text{ is strictly proper and stable and } F(0) = \mathbb{I} \tag{15}$$
$$(ii)\ \ F(s)H_0^{-1}(s) \text{ are proper and stable ;} \tag{16}$$
$$(iii)\ \ \|\bar{G}\|_{\mathscr{L}_1} L < 1 , \tag{17}$$

where the transfer function $\bar{G}(s)$ is defined by

$$\bar{G}(s) = H(s)(\mathbb{I} - F(s)) , \tag{18}$$

$H_0(s) = CH(s)$, $H(s) = (s\mathbb{I} - A_m)^{-1} B$ and

$$L = \max_{K_x \in \mathscr{K}_x} \|K_x\|_{\mathscr{L}_1} . \tag{19}$$

Remark 1 (Design of the control law): The simplest way of choosing $D(s)$ is to consider $D(s) = D_i(s)\mathbb{I}$ and consequently, $F(s) = F_i(s)\mathbb{I}$ with $F_i(s) = \frac{k_u k_d D_i(s)}{1 + k_u k_d D_i(s)}$. Moreover, depending on the relative degree of $H_0(s)$ one can have, for instance, $D_i(s) = \frac{1}{s}$ with relative degree $\rho = 1$, or $D_i(s) = \frac{1}{s^2}$ and $D_i(s) = \frac{3a^2 s + a^3}{s^3 + 3as^2}$ with $\rho = 2$.

Remark 2: It can be seen that the problem of finding $D_i(s)$ to generate $F_i(s)$ is a root locus problem, that always yields real and stable closed loop poles if $\rho = 1$ and stable poles (possibly imaginary) for $\rho = 2$. However, when $\rho > 2$ there is always a constant c such that if the gain $k_u k_d > c$ the function $F_i(s)$ is unstable. Moreover, for $\rho \leq 2$, it can be seen that if the gain $k_u k_d$ tends to infinity, then the poles of the closed loop system $F_i(s)$, although stable, also tend to infinity, yielding implementation problems.

A. Analysis of the $\mathscr{L}_1$ Adaptive Controller

With the introduction of the input filter $F(s)$, the predictor can no longer be used to evaluate the performance of the resultant closed loop system. The following reference system is introduced in order to provide the tools for performance analysis.

1) Stability of the Reference System: For performance evaluation of the $\mathscr{L}_1$ adaptive controller, the following closed-loop reference system is considered, which depends upon the ideal parameters k_u, $K_x(t)$ and $\mathbf{k}_\mathbf{w}(t)$:

$$\dot{\mathbf{x}}_{ref}(t) = A_m \mathbf{x}_{ref}(t) + B\left(k_u \mathbf{u}_{ref}(t) + \mathbf{r}_1(t)\right) \tag{20}$$
$$\mathbf{y}_{ref}(t) = C\mathbf{x}_{ref}(t) \quad , \quad \mathbf{x}_{ref}(0) = \mathbf{x}_0 \tag{21}$$
$$U_{ref}(s) = -k_d D(s) \bar{R}_{ref}(s) \tag{22}$$
$$\bar{\mathbf{r}}_{ref}(t) = k_u \mathbf{u}_{ref}(t) + \mathbf{r}_1(t) - K_g \mathbf{r}(t) \tag{23}$$

where $\mathbf{r}_1(t) = K_x(t)\mathbf{x}_{ref}(t) + \mathbf{k}_w(t)$ and $K_g \in \mathbb{R}^{n_u \times n_u}$ is a constant matrix. The following Lemma establishes the conditions for the stability of this closed-loop reference system and its proof can be found in [6].

Lemma 1: The reference system (20)-(23) is stable if k_d and $D(s)$ satisfy the conditions (15)–(17).

2) Guaranteed Transient Performance: The transient performance bounds for the $\mathscr{L}_1$ adaptive closed loop system are given in the following theorem.

Theorem 1 (Transient Performance): Given the system (10), the reference system (20)-(23) and the $\mathscr{L}_1$ adaptive controller (11), (12) and (13), subject to (15)-(17), we have

$$\|\tilde{\mathbf{x}}\|_{\mathscr{L}_\infty} \leq \gamma_0 \tag{24}$$
$$\|\mathbf{x} - \mathbf{x}_{ref}\|_{\mathscr{L}_\infty} \leq \gamma_1 \tag{25}$$
$$\|\mathbf{y} - \mathbf{y}_{ref}\|_{\mathscr{L}_\infty} \leq \|C\|_{\mathscr{L}_1} \gamma_1 \tag{26}$$
$$\|\mathbf{u} - \mathbf{u}_{ref}\|_{\mathscr{L}_\infty} \leq \gamma_2 \tag{27}$$

where

$$\gamma_0 = \left(\frac{\theta_m}{\gamma \lambda_{\min}(P)}\right)^{\frac{1}{2}} \tag{28}$$
$$\theta_m = 4\frac{\lambda_{\max}(P)}{\lambda_{\min}(Q)}\theta_1 + \theta_2 \tag{29}$$
$$\theta_1 = 4\left(\max_{K_x \in \mathscr{K}_x} \|K_x\|_2\right) d_{kx} + 4\Delta_0 d_{kw} \tag{30}$$
$$\theta_2 = 4\left(\max_{K_x \in \mathscr{K}_x} \|K_x\|_2 + \max_{k_u \in \mathscr{K}_u} \|k_u\|_2 + \Delta_0\right) \tag{31}$$
$$\gamma_1 = \frac{\|F_1\|_{\mathscr{L}_1} \gamma_0}{1 - \|\bar{G}\|_{\mathscr{L}_1} L} \tag{32}$$
$$\gamma_2 = \|k_u^{-1} F\|_{\mathscr{L}_1} L\gamma_1 + \|F_2\|_{\mathscr{L}_1} \gamma_0 \tag{33}$$
$$F_1(s) = H(s)F(s)H_0^{-1}C \tag{34}$$
$$F_2(s) = k_u^{-1} F(s) H_0^{-1} C . \tag{35}$$

The proof for this result can be found in [6]. Thus, if the adaptation rate γ is selected sufficiently large, the closed-loop system follows the reference system not only asymptotically, but also during the transient phase. This reduces the design problem to that of finding $D(s)$ and k_d, such that the conditions (15)-(17) hold and the closed-loop reference system (20)-(23) has the desired response.

B. Design Guidelines

Bearing in mind that the reference system and its control law $\mathbf{u}_{ref}(t)$ depend upon the ideal values of the unknown parameters and are therefore not implementable, it is important to understand how the bounds established in Theorem 1 can be used to ensure the desired closed loop system response.

Notice that the ideal control law is given by

$$k_u \mathbf{u}_{id}(t) = K_g \mathbf{r}(t) - K_x(t)\mathbf{x}_{id}(t) - \mathbf{k}_w(t) \tag{36}$$

which leads to the closed loop ideal system

$$\dot{\mathbf{x}}_{id}(t) = A_m \mathbf{x}_{id} + B(k_u \mathbf{u}_{id}(t) - K_x(t)\mathbf{x}_{id}(t) - \mathbf{k}_w(t)) = A_m \mathbf{x}_{id} + BK_g \mathbf{r}(t) \tag{37}$$
$$\mathbf{y}_{id} = C\mathbf{x}_{id} \quad , \quad \mathbf{x}_{id}(0) = \mathbf{x}_0 , \tag{38}$$

by canceling the uncertainties exactly. Conversely, in the case of the closed-loop reference system (20)-(23), the control law

is a low-pass filtered version of $\mathbf{u}_{id}$. As in [11], it can be seen that the response of the closed loop reference system can be made arbitrarily close to the one of the ideal system by increasing the bandwidth of $F(s)$, i. e., as $F(s) \to \mathbb{I}$ then $\|\mathbf{y}_{ref} - \mathbf{y}_{id}\|_{\mathscr{L}_\infty} \to 0$. Increasing the bandwidth of $F(s)$ may affect the robustness of the closed loop, as proven in [5], and therefore a trade-off must be found to obtain the desired performance and robustness bounds, which can be addressed using well-known tools from classical and robust control theory.

IV. SIMULATION RESULTS

In this section the implementation details and the simulation results obtained with the inner loop $\mathscr{L}_1$ controller, along a typical rotorcraft maneuver, are presented and discussed.

The main implementation aspects focused hereafter are the definition of the bounds for $\hat{k}_u$, $\hat{K}_x$ and $\hat{\mathbf{k}}_w$, and also the design of the filter $F(s)$. For the computation of the projection bounds for the adaptive parameters, the region of operation for the helicopter is considered to be defined by the set $\Xi = \{\xi \in \mathbb{R}^4 | \xi_1 \in [\underline{\xi}_1, \overline{\xi}_1], \xi_2 = \xi_3 = 0, \xi_4 = \pi/2\}$, where $\xi = [V_c \; \gamma_c \; \dot{\psi}_c \; \psi_{ct}]'$, $\underline{\xi}_1 = 0.75$ and $\overline{\xi}_1 = 1.25$. The control effectiveness parameter $\hat{k}_u(t)$ was initialized with $\hat{k}_u(0) = 1$ and its adaptation interval for projection was set to $\mathscr{K}_u = \{k_u \in \mathbb{R} \,|\, \underline{k}_u \leq k_u \leq \underline{k}_u\}$, where $\underline{k}_u = 0.75$ and $\overline{k}_u = 1.25$, which correspond to a loss/gain of 25% of controller effectiveness. The adaptive parameter matrix $\hat{K}_x(t)$ was initialized at $\hat{K}_x(0) = K_n$, while its bounds were defined by the set $\mathscr{K}_x = \{K_x \in \mathbb{R}^{n_u \times n_x} | \underline{k}_{x_{ij}} \leq K_{x_{ij}} \leq \overline{k}_{x_{ij}} \;,\; \forall_{i=1,\ldots,n_u \,,\, j=1,\ldots,n_x}\}$, where $\overline{k}_{x_{ij}}$ and $\underline{k}_{x_{ij}}$ are the lower and upper bounds for each element of $\hat{K}_x(t)$. These bounds are computed from the nominal controller K_n, which is a stabilizing controller for all plants within the region of operation, by setting $\overline{k}_{x_{ij}} = -\underline{k}_{x_{ij}} = 2\,|k_{n_{ij}}|$. Also, the upper bound for the adaptation parameter matrix is given by $L = \max_{K_x \in \mathscr{K}_x} \|K_x\|_{\mathscr{L}_1} = 2\,\|K_n\|_{\mathscr{L}_1} = 0.2306$. The uncertainty adaptation parameter $\hat{\mathbf{k}}_w$ was initialized as $\hat{\mathbf{k}}_w(0) = \mathbf{0}$ and its bounds were defined by the set $\mathscr{K}_w = \{k_w \in \mathbb{R} \,|\, |k_{w_i}| \leq 0.5 \;,\; \forall\, i = 1, \ldots, n_u\}\}$. The matrices A_n and B were computed for the central point of the region of operation defined above. The choice of A_n, B and K_n follow from the methodology described in [1].

The output signal was defined as $\mathbf{y}(t) = [\; \mathbf{v}'_B(t) \quad \omega_{B_3}(t) \;]' \in \mathbb{R}^4$, the reference signal $\mathbf{r}(t) = \mathbf{0}$ and $H_0(s)$ yields a 4×4 stable and proper transfer function matrix with stable transmission zeros. Noting that $\|H\|_{\mathscr{L}_1} = 263.68$, to satisfy condition (17), the filter $F(s)$ can be defined by considering $D(s) = \frac{1}{s}\mathbb{I}$ and taking into account the set $\mathscr{K}_u$, yielding two different filters: $\underline{F}(s) = (\mathbb{I} + \underline{k}_u k_d D(s))^{-1} \underline{k}_u k_d D(s)$ and $\overline{F}(s) = \left(\mathbb{I} + \overline{k}_u k_d D(s)\right)^{-1} \overline{k}_u k_d D(s)$, from which $\bar{G}_1(s) = H(s)\,(\mathbb{I} - \underline{F}(s))$ and $\bar{G}_2(s) = H(s)\,(\mathbb{I} - \overline{F}(s))$ can be obtained. Thus, the value of k_d from which condition (17) is satisfied can be computed by evaluating $\|\bar{G}_1\|_{\mathscr{L}_1} L$ and $\|\bar{G}_2\|_{\mathscr{L}_1} L$ yielding the condition $k_d \geq 273$, obtained iteratively using Matlab. In the simulation results the value $k_d = 280$ was used, for which $\|\bar{G}_1\|_{\mathscr{L}_1} L = 0.606$ and $\|\bar{G}_2\|_{\mathscr{L}_1} L = 0.975$. The adaptive gain γ was set to $\gamma = 10000$.

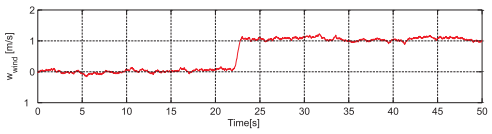

Fig. 1. Wind velocity disturbance in the inertial frame (only the z-axis component is shown).

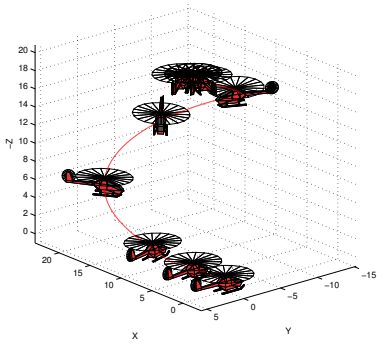

Fig. 2. $\mathscr{L}_1$ controlled trajectory.

The simulation results herein presented were obtained using the full nonlinear dynamic model SimModHeli, parameterized for the Vario X-Treme model-scale helicopter, within the Matlab/Simulink simulation environment. The rotorcraft is required to track the following trajectory: (i) a straight line moving sideways ($V_c = 1$ m/s, $\psi_{ct} = \pi/2$ rad and $\dot{\psi}_c = \gamma_c = 0$); (ii) followed by a helix keeping the nose of the helicopter pointing to the center of the helix and doubling the linear speed ($V_c = 2$ m/s, $\psi_{ct} = \pi/2$ rad, $\dot{\psi}_c = 0.24$ rad/s and $\gamma_c = 0.34$ rad); and finally (iii) hover at a specific point ($\psi_{ct} = \pi/2$ rad and $V_c = \dot{\psi}_c = \gamma_c = 0$). The initial state vector is $\mathbf{x}_0 = \mathbf{0}$. To evaluate the behavior of the closed-loop system in realistic operation scenarios wind disturbances were included in all linear velocity channels. The disturbances were generated using the Von Karman wind model and also a discrete wind gust with amplitude 1 m/s, rising time of 1s, applied at time $t = 22$s (see [7] and references therein for further insight). The z-axis component of wind disturbance is displayed in Figure 1.

The trajectory described by the rotorcraft nonlinear simulation model in closed-loop $\mathscr{L}_1$ adaptive system is depicted in Figure 2. The remaining simulation results, presented in Figure 3, compare the performance obtained with the $\mathscr{L}_1$ adaptive controller with that obtained with the fixed nominal state feedback controller K_n computed as in [1]. It can be seen that the $\mathscr{L}_1$ adaptive controller displays considerably smaller errors than the nominal controller K_n. The nominal controller has an acceptable performance in the first part of the trajectory (that would belong to the predefined region of operation if there was no wind disturbance), but in the rest of the reference trajectory, its performance is poor failing to follow the reference signals and rejecting the wind gust. The $\mathscr{L}_1$ adaptive controller is able to reject

the wind induced disturbances, keeping the vehicle close to the reference velocities, even when it operates far form the design conditions. From the figures it can be easily concluded that the performance of the $\mathscr{L}_1$ surpasses that of the linear controller showing the clear advantages of fast adaptation.

V. CONCLUSIONS

This paper presented the design and performance evaluation of a high bandwidth inner loop $\mathscr{L}_1$ adaptive controller to provide attitude and velocity stabilization of an autonomous rotorcraft in the presence of wind disturbance.

The nonlinear dynamic model of the rotorcraft was written as a linear time-varying system for a predefined region of operation, for which an $\mathscr{L}_1$ adaptive controller was designed. The effectiveness of the proposed control laws was assessed in the MATLAB/Simulink simulation environment with the full nonlinear model of the rotorcraft using demanding reference signals and wind disturbances, generated using Von Karman models and wind gusts. The results obtained indicate that the proposed methodology can provide better performance than that achieved by the controller used to specify the reference system, following demanding reference signals while rejecting the wind disturbances.

Further research effort shall focus on the position control of the autonomous rotorcraft.

REFERENCES

[1] B. Guerreiro, C. Silvestre, R. Cunha, and D. Antunes, "Trajectory tracking $\mathscr{H}_2$ controller for autonomous helicopters: and aplication to industrial chimney inspection," in *17th IFAC Symposium on Automatic Control in Aerospace*, Toulouse, France, June 2007.

[2] C. Cao and N. Hovakimyan, "$\mathscr{L}_1$ adaptive controller for systems with unknown time-varying parameters and disturbances in the presence of non-zero trajectory initialization error," *International Journal of Control*, vol. 81, no. 7, pp. 1148–1162, 2008.

[3] ——, "$\mathscr{L}_1$ adaptive output feedback controller for systems of unknown dimension," *IEEE Transactions on Automatic Control*, vol. 53, no. 3, pp. 815–821, 2008.

[4] ——, "Design and analysis of a novel $\mathscr{L}_1$ adaptive control architecture with guaranteed transient performance," *IEEE Transactions on Automatic Control*, vol. 53, no. 2, pp. 586–591, 2008.

[5] ——, "Stability margins of $\mathscr{L}_1$ adaptive controller: Part ii," in *In Proceedings of American Control Conference*, New York City, USA, July 2007.

[6] ——, "$\mathscr{L}_1$ adaptive controller for multi-input multi-output systems in the presence of unmatched disturbances," in *American Control Conference*, Seattle, WA, June 2008, pp. 4105–4110.

[7] G. D. Padfield, *Helicopter Flight Dynamics: The Theory and Application of Flying Qualities and Simulation Modeling*, ser. AIAA Education Series. Washington DC: AIAA, 1996.

[8] R. Cunha, "Modeling and control of an autonomous robotic helicopter," Master's thesis, Department of Electrical and Computer Engineering, Instituto Superior Técnico, Lisbon, Portugal, May 2002.

[9] R. Cunha, B. Guerreiro, and C. Silvestre, "Vario-xtreme helicopter nonlinear model: Complete and simplified expressions," Instituto Superior Técnico, Institute for Systems and Robotics," Technical Report, 2005.

[10] J. B. Pomet and L. Praly, "Adaptive nonlinear regulation: Estimation from the lyapunov equation," *IEEE Transactions on Automatic Control*, vol. 37, no. 6, pp. 729–740, June 1992.

[11] C. Cao and N. Hovakimyan, "Guaranteed transient performance with $\mathscr{L}_1$ adaptive controller for systems with unknown time-varying parameters: Part i," in *In Proceedings of American Control Conference*, New York City, USA, June 2007.

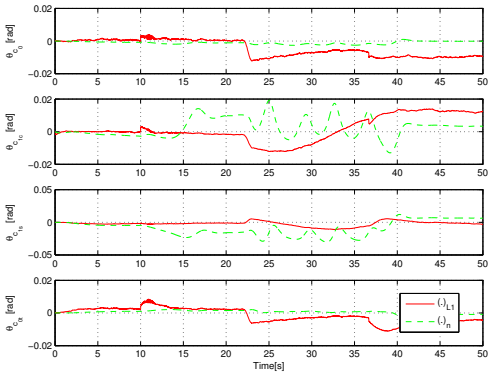

(a) Actuation Error

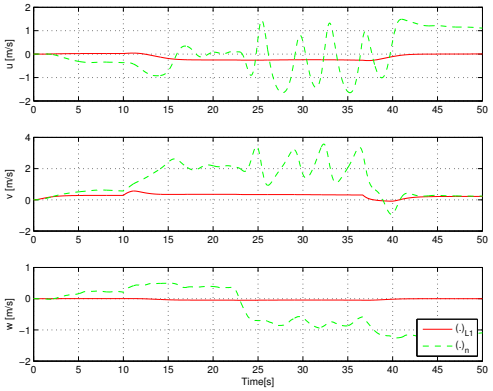

(b) Linear Velocity Error

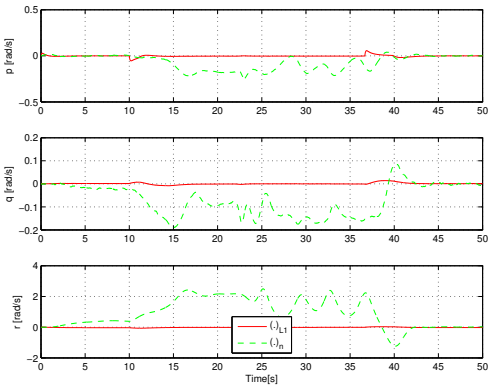

(c) Angular Velocity Error

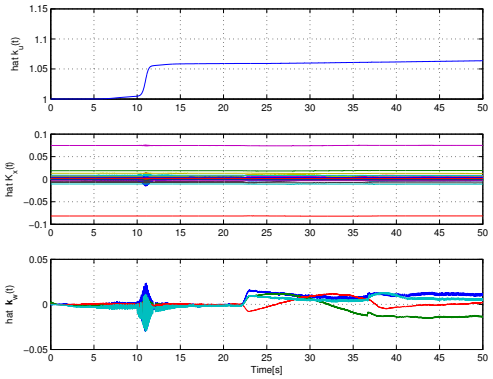

(d) $\mathscr{L}_1$ Parameters Evolution

Fig. 3. Simulation results.